Proceedings of the ASME 2014 33rd International Conference on Ocean, Offshore and Arctic Engineering
OMAE2014
June 8-13, 2014, San Francisco, USA

OMAE2014-23475

MODELING AND ANALYSIS OF A MULTI DEGREE OF FREEDOM POINT ABSORBER WAVE ENERGY CONVERTER

Andrew F. Davis
Department of Mechanical Engineering
University of Washington
Seattle, Washington 98195
Email: afdavis@uw.edu

Jim Thomson
Applied Physics Laboratory
University of Washington
Seattle, Washington, 98195
Email: jthomson@apl.washington.edu

Tim R. Mundon
Oscilla Power Inc.
Seattle, Washington, 98103
Email: mundon@oscillapower.com

Brian C. Fabien
Department of Mechanical Engineering
University of Washington
Seattle, Washington, 98195
Email: fabien@uw.edu

ABSTRACT

This paper illustrates an approach to the modeling of a point absorbing Wave Energy Converter (WEC) with the intent of analyzing the sensitivity of the system response to variation in the model parameters. Using first principles, the nonlinear equations of motion are formed to describe the heave motion of a 3 body system. A linearized model is developed and used to simulate the system in both the time and frequency domains. The input to the model is a time series displacement and a time series velocity that describes the incident waves. A sensitivity analysis is then performed on the system parameters to show how the characteristics of the heave plate, the component masses, and the mass of the entrained fluid affect the performance of the system. The model is validated by numerically modeling a generation 1 device produced by Oscilla Power Inc., which is compared against experimental data from a field test on Lake Washington. The WEC is designed to provide tension along a series of tethers with connected power take off units. The wave input is specified using frequency spectra measured with a nearby Datawell Waverider MK III buoy during the field testing, from which time domain waves are reconstructed.

INTRODUCTION

Wave energy has strong potential for being a component of the solution to the problems presented by an increasing energy demand. While the idea of harvesting energy from waves is not new, there has been increasing research in this area. Wave energy converters (WECs) have significant potential in the marine renewable energy field, and pre-commercial prototypes of marine energy devices are being developed and implemented in test situations. However, significant research is still required to develop wave energy into a feasible renewable energy source for coastal regions [1].

The mooring and installation of a wave energy converter is a significant factor in the cost of produced energy. In shallow waters (i.e., depth less than 30 meters) it may be cost effective to use a rigid foundation, such as a monopile or jacketed pile. However at greater depths or when the wave energy converter must respond dynamically to the water surface (as in the case of point absorbing wave energy converters), compliant moorings are necessary. Work has been done to model the dynamics of compliant and even slack mooring lines [2]. However, this must be combined with an effective model of WEC dynamics and power

generation in order to optimize the configuration of the mooring lines to minimize the cost of power production.

There are several existing commercial software packages such as OrcaFlex, ProteusDS, ANSYS Aqwa, and WAMIT to model the dynamics of marine systems. However, by extending a first principles model to arrays of WECs it will be possible to create simple and generic design tools to maximize the performance of marine energy converters. To better understand the performance of the system, and thereby work towards the eventual goal of performance maximization, the final outcome of the system modeling and identification is the parameter sensitivity analysis.

Section 1 presents a general description and the simplifying assumptions that are used to formulate the equations of motion. Section 2 gives a brief description of the deployment of the prototype WEC along with the experimental resources used for validation wherein a representative wave period and amplitude are used to realistically describe the behavior of the lake deployment. In section 3 the numerical methods used to solve for the dynamics of the WEC are shown, then the simulated output and the experimental data is compared. Section 4 develops conclusions on which parameters have the greatest effect on the efficiency of the system. The study is concluded with a discussion of results in section 5. Finally, the directions of future study are presented in section 6.

1 SYSTEM MODEL

The Oscilla WEC is a point absorbing wave energy converter that produces power from the rate of change of tension in the power take off (PTO) units. The simplified model presented assumes that the deflection in the PTOs and the load cell is negligible compared to the deflection in the connections between the WEC components. Because the mooring lines are placed symmetrically, and are not exerting significant tension, this initial model does not include the mooring lines. Considering the vertical motion of the buoy while neglecting the force component of the mooring lines can still produce a reasonably accurate simulation [3].

Figure 1 shows a simplified model of the prototype point absorber. Component displacements are shown from the natural length of each connection. The variable y_w is the distance from the steady water line to the surface of the water. The displacements y_b, y_p, and y_h show the positive direction of motion for the buoy, PTO units, and heave plate, respectively. Velocities are denoted with a single dot and accelerations are denoted with two dots. The variables K_{r1} and K_{r2} are the linear spring constants that are used to model the connections between the lumped mass components. The variables L_1 and L_2 denote the lengths of the connections between the buoy and the load cell and the lower PTO unit and the heave plate respectively. For the deployed system $L_2 >> L_1$.

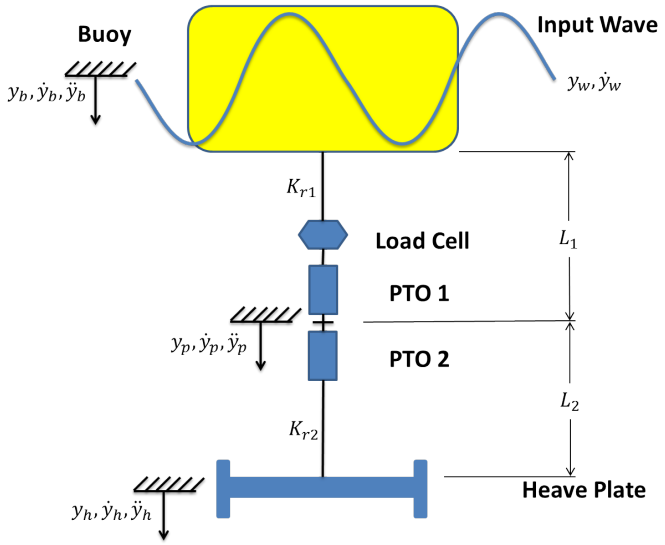

FIGURE 1. Simplified model of the Oscilla Power prototype WEC.

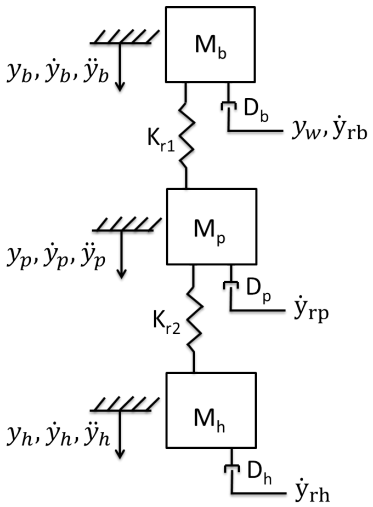

FIGURE 2. Mass-Spring-Damper model of the Oscilla Power prototype.

The buoy and components will follow the motion of the wave, and the heave plate will create a significant amount of tension in the PTO units. The mass of the heave plate, as it is submerged some distance below the surface, is subject to a greatly reduced wave forcing and its drag and inertia are large enough so that there will always be tension in the central cable. By continuously maintaining tension in the cable, destructive shock loading is avoided during deployment.

While Ref. [3] presents a similar system description to Figs.

1 and 2, it is important to note that in Ref. [3] both bodies breach the surface which results in two variable buoyant forces compared to the single variable buoyant force in this model. The PTO connection in Ref. [3] produces a damping force proportional to the relative velocity, whereas in this model the PTO force is modeled as a linear spring as shown in Fig. 2. In Ref. [3] the forces associated with the radiation damping of the system are computed using a state space formulation, by contrast, this model only considers the profile drag and skin friction on each body. Finally, [3] uses the commercial package, WADAM, to compute coupled added mass terms and produce the numerical validation of the model, whereas this development uses simplified body geometry to estimate the added mass and performs the validation against experimental results.

1.1 EQUATIONS OF MOTION

A simplified model of a mass-spring-damper system is created to represent the system shown in Fig. 1. Figure 2 shows how the WEC is modeled as 3 separate masses with the connections between each mass acting as springs. The displacements and spring constants are defined in Fig. 1. The variables M_b, M_p, and M_h are the lumped masses of the buoy, PTO units, and the heave plate, respectively. The linear drag coefficients, D_b, D_p, and D_h, are shown on each mass in reference to the relative water velocity. The relative water velocity of the buoy, $\dot{y}_{rb}$, the PTO units, $\dot{y}_{rp}$, and the heave plate, $\dot{y}_{rh}$, is given by an exponential attenuation term that models a diminishing water velocity as a function of the wave number and depth. The water displacement, y_w, is shown in reference to the buoy because the surface of the wave and the buoy displacement are measured from the same reference and the wave displacement is used to compute the variable buoyant force acting on the buoy.

The primary source of damping in the system is the fluid drag of the masses passing through the water. The dynamics of the WEC are decomposed and analyzed in a similar manner to Refs. [4,5]. By lumping the load cell and both PTO units together as a single mass the number of equations of motion is reduced from 5 to 3 with little loss of detail. The PTO lumped mass is a reasonable approximation because the load cell and PTO units are connected with rigid links with no appreciable strain. Therefore, the displacements of the 3 smaller components are all the same as the lumped displacement y_p.

Using Newton's law to describe the equation of motion for each mass results in 3 second order ordinary differential equations. The equation of motion for each of the three masses takes the form

$$\begin{aligned} m\ddot{y} =& F_{Weight} + F_{Buoyancy} + F_{Drag} + F_{Spring} \\ &+ F_{Radiation} + F_{WaveExcitation}, \end{aligned}$$

where the dot notation shows the number of time derivatives of a variable and the product of the mass and acceleration is equal to the sum of the forces acting on the mass.

The weight and buoyancy of each mass are included in the summation of forces according to the direction conventions established in Fig. 1. It is important to note that the buoy will have a variable buoyant force, whereas the other components will have a constant buoyant force. The variation in the buoyant force at the buoy is due to the fact that as more of the buoy becomes submerged the weight of the displaced fluid will increase which causes the buoyant force to increase.

The drag force is comprised of two main components, the friction drag and the profile drag. The drag force acting on a mass passing through a fluid is computed using the equation

$$F_{Drag} = \frac{1}{2} C_{drag} A \rho V |V|, \tag{1}$$

where C_{drag} is the coefficient of drag, the computed area, A, is the area relevant to the type of drag, V is the net velocity of the object with respect to the fluid particles surrounding it, and ρ is the density of the fluid. The friction drag coefficient, C_f, is computed by

$$C_f = \frac{0.16}{Re^{1/7}}, \tag{2}$$

$$Re = \frac{\hat{a}}{2} \frac{\omega d}{\nu}, \tag{3}$$

where Re is the Reynolds number computed in wave conditions, $\hat{a}$ is the peak to peak amplitude of the wave, d is the characteristic length of the buoy, ω is the frequency, and ν is the kinematic viscosity of the water [6]. For the system simulated below a characteristic length of 1.7 meters is used. Equation (2) computes the average shear stress coefficient which is used as the coefficient of skin friction. Small amounts of friction will be generated by the boundary layer effects as the water travels along the sides of the masses. Once the coefficient of skin friction, C_f, is computed Eqn. (1) is used to compute the force acting on the mass.

The second type of drag is the profile drag, which is created when an object passes through a fluid, requiring fluid particles to pass around the mass. Equation (1) is also used to compute the profile drag on each mass by using a dimensionless drag coefficient, C_D, and the projected surface area of the mass in the direction of motion. The dimensionless drag coefficients are determined using the shape and the dimension ratios of each mass [7].

Both forms of drag are computed using the relative velocity between the mass and the fluid. To accurately characterize the fluid velocity at each point in the model an attenuation term is used to describe the water particle velocity surrounding each mass. This is given by $e^{-(depth)(k)}$, where $k = \frac{\omega^2}{g}$ is the wave

number [8]. The wave number is an expression of the wave frequency, ω, and the gravitational acceleration, g.

For the system considered below, the wave period that was used to compute the wave frequency is 3 seconds. While 3 seconds is a very small wave period for ocean waves, 3 seconds is a reasonable period in Lake Washington. The exponential attenuation term computes a very small velocity at the depth of the PTO units and by extension the wave velocity at the depth of the heave plate is negligible during operational conditions. Figure 2 illustrates that each mass will have a different surrounding water particle velocity that will be used when computing the drag. The attenuated wave velocities are computed as

$$\dot{y}_{rb} = \dot{y}_w e^{-\frac{1}{2}k},$$
$$\dot{y}_{rp} = \dot{y}_w e^{-7k},$$
$$\dot{y}_{rh} = \dot{y}_w e^{-14k}.$$

The attenuated wave velocities are approximated using constant values for the depths for each mass. A constant depth of $\frac{1}{2}$ meter is used for the buoy, 7 meters for the lumped PTO units, and 14 meters for the depth of the heave plate. Calculating the wave particle velocity attenuation as if each body is a single point is valid in situations where the bodies are small compared to the depth that the wave motion penetrates the water.

For this model the spring force, F_{Spring}, is given as a linear spring constant, K_{r1} or K_{r2}, multiplied by the net extension from the connections natural length to compute the spring force acting on each mass. The spring constant K_{r2} is given by the vendor estimation of the rope used, and K_{r1} is large enough to ensure that the buoy and the PTO mass move together. Since the displacements are measured from the natural length rather than from a single reference point, the net extension is computed by finding the difference of the displacements of each body.

The radiation damping term, $F_{Radiation}$, is comprised of both an added mass term and a radiation damping term. The radiation damping term is a force that acts on the buoy during oscillatory motion in the water. Since the WEC has a very small characteristic length compared to the wavelength the radiation damping term is insignificant [6]. By contrast the added mass of the system still plays a significant role in the formulation of the equations of motion and is described below. The added mass of each body is summed with the dry mass to create a single term to describe the inertia of each body.

The heave response of an axisymmetric body when the draft of the buoy is small compared to the wavelength is $z(t) = a\cos(\omega t + \varepsilon)$, where $z(t)$ is the heave displacement of the body, a is the amplitude, ω is the wave frequency, t is the time, and ε is the phase of the response [6]. The wave excitation force on the buoy can be modeled similarly to [5], as $F_{excitation} = aF\cos(\omega t + \varepsilon)$. Just as in [5] the phase is assumed to be zero and in this case, $F = B_b$, where B_b is referred to as the variable buoyancy. B_b has units of force per unit length and is given by multiplying the area of the bottom of the buoy by the density of water and the acceleration due to gravity. When B_b is multiplied by the length of the submerged portion of the buoy the weight of the displaced fluid is the same as the buoyant force acting on the buoy. The excitation force is shown in the equation of motion as $F_{WaveExcitation} = B_b y_w$, where y_w is the position of the wave surface described in further detail in section 3.1. The wave excitation on the PTO units and the heave plate is negligible because they are submerged several meters below the wave motion.

Three separate equations of motion are formed to describe the independent motion of all three lumped masses. The Oscilla system has a significantly more rigid connection between the buoy and the PTO units than the connection between the PTO units and the heave plate. This is reflected in the model by the use of the two different spring constants K_{r1} and K_{r2}. Nevertheless, three equations of motion are modeled because it is the goal of this research to evaluate how variations in the structural properties affect the power production of the system. The resulting differential equations are:

$$\begin{aligned} m_{vb}\ddot{y}_b =& B_b y_w + m_b g - B_b y_b - \frac{C_{Db}}{2} A_b \rho (\dot{y}_b - \dot{y}_{rb})|\dot{y}_b - \dot{y}_{rb}| \\ & - \frac{C_f}{2} A_{bwet} \rho (\dot{y}_b - \dot{y}_{rb})|\dot{y}_b - \dot{y}_{rb}| - K_{r1}(y_b - y_p), \quad (4) \\ m_{vp}\ddot{y}_p =& m_p g - B_p - \frac{C_{Dp}}{2} A_p \rho (\dot{y}_p - \dot{y}_{rp})|\dot{y}_p - \dot{y}_{rp}| \\ & - \frac{C_f}{2} A_{pwet} \rho (\dot{y}_p - \dot{y}_{rp})|\dot{y}_p - \dot{y}_{rp}| \\ & - K_{r1}(y_p - y_b) - K_{r2}(y_p - y_h), \quad (5) \\ m_{vh}\ddot{y}_h =& m_h g - B_h - \frac{C_{Dh}}{2} A_h \rho (\dot{y}_h - \dot{y}_{rh})|\dot{y}_h - \dot{y}_{rh}| \\ & - \frac{C_f}{2} A_{hwet} \rho (\dot{y}_h - \dot{y}_{rh})|\dot{y}_h - \dot{y}_{rh}| - K_{r2}(y_h - y_p). \quad (6) \end{aligned}$$

The inertia term in the equation of motion for the buoy, Eqn. (4), is $m_{vb}\ddot{y}_b$, where m_{vb} is the virtual mass of the buoy described later, and $\ddot{y}_b$ is the acceleration of the buoy defined in Figs. 1 and 2. The weight of the buoy is given as $F_{Weight} = m_b g$, where m_b is the mass of the buoy given in Tab. 1 and $g = 9.81\frac{m}{s^2}$ is the acceleration due to gravity at sea level. $F_{Buoyancy} = B_b y_b$ is the variable buoyant force of the buoy described above.

The total drag force is given by summing the friction drag and the profile drag. The drag force is included in the equation of motion as

$$\begin{aligned} F_{Drag} =& \frac{C_{Db}}{2} A_b \rho (\dot{y}_b - \dot{y}_{rb})|\dot{y}_b - \dot{y}_{rb}| \\ & + \frac{C_f}{2} A_{bwet} \rho (\dot{y}_b - \dot{y}_{rb})|\dot{y}_b - \dot{y}_{rb}|, \end{aligned}$$

where C_{Db} is the drag coefficient based on the geometry of the leading surface of the buoy as it moves in the positive direction. A_b is the projected area of the buoy's leading surface, for this model the magnitude of the drag force is computed identically for positive and negative velocities. The variable, ρ, is the density of the surrounding fluid, and the difference $(\dot{y}_b - \dot{y}_{rb})$ is the relative velocity of the buoy. C_f is the shear stress coefficient from Eqn. (3) and is assumed to be identical for all three lumped masses. A_{bwet} is the submerged surface area of the sides of the buoy. For the buoy the wetted area is given by a constant surface area, just as with the other two lumped masses, to preserve the linearity of the model.

Finally, the spring force in Eqn. (4) is given by $F_{Spring} = K_{r1}(y_b - y_p)$, where $y_b - y_p$ is the net extension in the connection between the buoy and the PTO units and K_{r1} is the spring constant of the connection between the buoy and the PTO units as shown in Figs. 1 and 2. The sign conventions that appear in the equations of motion are established in Fig. 1, and subscripts defined in Figs. 1 and 2 are used to distinguish specific components. The other equations of motion are developed in a similar manner to the Eqn. (4).

It is important to note that the virtual mass is denoted with m_{vb}, m_{vp}, and m_{vh} where the subscript v identifies that the value is the virtual mass and the bodies are identified with subscripts b, p, and h. The virtual mass for each component is the sum, $m_v = m + m_a$, where m_a is the added mass correction factor and m is the mass. The added mass term is used to compensate for the fluid that is carried along with each mass as the components pass through the water. This entrained fluid may be a substantial modification to the inertia of each component, however it is important to note that this added mass does not contribute to the weight of the components.

When computing the added mass in the heave direction the geometry of the bodies is required. Typically a tool such as WAMIT is used to determine added mass coefficients for bodies with complex geometries. However, in this paper the geometries of the bodies are simplified and closed form equations for added mass are given in Ref. [9]. In particular the added mass for the PTO unit is roughly 4% of the actual mass and the added mass of the heave plate and buoy are roughly 40% of their respective masses. The hydrodynamic mass of the vertical motion of a circular disk, which represents the heave plate, is given by the expression $m_h = 8/3\rho r^2$, where ρ is the density and r is the radius of the disk. The added mass of the PTO units is computed in a similar manner to the added mass of the heave plate. For the model validated below the added mass of the buoy is computed by taking into consideration the volume of water displaced as a result of the buoy motion. The sensitivity study shows the effect of changes in the added mass of each body.

1.2 FREQUENCY RESPONSE ANALYSIS

In order to develop the spectral method of simulating the response of the system the nonlinear drag term is linearized. Damping coefficients are often a very uncertain component of a model, in this case the dominant wave period of roughly 2.5 seconds is used and a peak to peak amplitude of 1 meter is used. By choosing a somewhat larger than standard wave amplitude the linear approximation is guaranteed not to under estimate the damping throughout the full range of the velocity. An over estimation of the simplified damping term at this point in the model is acceptable considering that there are additional forms of damping, such as radiation damping, that would cause additional losses in a real system.

The following development of a linearized drag constant is shown for a general mass which is signified by parameters with no subscript (b, p, or h). C_D, A, A_{wet}, and C_f are the same parameters as described in section 1.1, however this drag coefficient linearization is performed for all 3 bodies. The nonlinear drag coefficient is composed of the profile drag and the skin friction

$$C = \frac{1}{2}C_D A\rho + \frac{1}{2}C_f A_{wet}\rho, \tag{7}$$

where the first term is the profile drag and the second term is the skin friction. In the case of the buoy A_{wet} is assumed to be half the surface area of the buoy to obtain a linear damping coefficient. The wetted areas of the other bodies are calculated based on geometry. By Ref. [10] the nonlinear damping can be approximated by

$$F_{damping} = C\dot{x}|\dot{x}| = C\hat{a}\omega_o\dot{x}, \tag{8}$$

where $\hat{a}$ and ω_o are the peak to peak amplitude and the wave frequency respectively, and $\dot{x}$ is the body velocity. The linear drag coefficient,

$$D = \frac{1}{2}\hat{a}\omega_o\left[C_D A_{body} + C_f A_{wet}\right], \tag{9}$$

is formed by using the velocity linearization in Eqn. (8) and summing both types of drag on the system. The drag force is modeled by $F_{Drag} = D\dot{x}$. The wave displacement, $y_w = a\,sin(\omega t)$, and wave velocity, $\dot{y}_w = a\,\omega\,cos(\omega t)$, are input forcing functions to this model described in further detail in section 3.1. The variables a and ω are the amplitude and frequency inputs determined by the Pierson-Moskowitz spectrum described in section 2. The terms are separated and organized for state space formulation as

follows:

$$\begin{aligned} m_{vb}\ddot{y}_b =& -D_b\dot{y}_b - B_b y_b - K_{r1}y_b + K_{r1}y_p + m_b g + B_b y_w \\ &+ D_b\dot{y}_{rb}, \quad (10) \\ m_{vb}\ddot{y}_p =& -D_p\dot{y}_p - K_{r1}y_p - K_{r2}y_p + K_{r1}y_b + K_{r2}y_h \\ &+ m_p g - B_p + D_p\dot{y}_{rp}, \quad (11) \\ m_{vh}\ddot{y}_h =& -D_h\dot{y}_h - K_{r2}y_h + K_{r2}y_p + m_h g - B_h + D_h\dot{y}_{rh}. \quad (12) \end{aligned}$$

The 3 degree of freedom system in state space format with the wave input is given by:

$$\underline{M}\ddot{y} = \underline{K}y + \underline{C}\dot{y} + e_o + e_1 y_w + e_2\dot{y}_w, \quad (13)$$

$$\underline{M} = \begin{bmatrix} m_b + m_{ab} & 0 & 0 \\ 0 & m_p + m_{ap} & 0 \\ 0 & 0 & m_h + m_{ah}, \end{bmatrix},$$

$$\underline{K} = \begin{bmatrix} -(B_b + K_{r1}) & K_{r1} & 0 \\ K_{r1} & -(K_{r1} + K_{r2}) & K_{r2} \\ 0 & K_{r2} & -K_{r2} \end{bmatrix},$$

$$\underline{C} = \begin{bmatrix} -D_b & 0 & 0 \\ 0 & -D_p & 0 \\ 0 & 0 & -D_h \end{bmatrix},$$

$$e_o = \begin{bmatrix} m_b g \\ m_p g - B_p \\ m_h g - B_h \end{bmatrix}, e_1 = \begin{bmatrix} B_b \\ 0 \\ 0 \end{bmatrix}, e_2 = \begin{bmatrix} D_b e^{-\frac{1}{2}k} \\ D_p e^{-7k} \\ D_h e^{-14k} \end{bmatrix}.$$

The virtual mass matrix, $\underline{M}$, is composed of diagonal elements where the mass and the added mass are summed. Let $q_1 = y$ and $q_2 = \dot{y}$ to perform a reduction of order. The new first order system is

$$\dot{q}_1 = q_2, \quad (14)$$

$$\dot{q}_2 = \underline{M}^{-1}\left[\underline{K}q_1 + \underline{C}q_2 + e_o + e_1 y_w + e_2\dot{y}_w\right]. \quad (15)$$

Using $q = \begin{bmatrix} q_1 \\ q_2 \end{bmatrix}$ the equations of motion become

$$\dot{q} = \hat{A}q + \hat{B}_o + \hat{B}_1 y_w + \hat{B}_2\dot{y}_w, \quad (16)$$

where

$$\hat{A} = \begin{bmatrix} 0 & I \\ \underline{M}^{-1}\underline{K} & \underline{M}^{-1}\underline{C} \end{bmatrix}, \hat{B}_o = \begin{bmatrix} zeros(3,1) \\ \underline{M}^{-1}e_o \end{bmatrix},$$

$$\hat{B}_1 = \begin{bmatrix} zeros(3,1) \\ \underline{M}^{-1}e_1 \end{bmatrix}, \hat{B}_2 = \begin{bmatrix} zeros(3,1) \\ \underline{M}^{-1}e_2 \end{bmatrix}, q = \begin{bmatrix} y_b \\ y_p \\ y_h \\ \dot{y}_b \\ \dot{y}_p \\ \dot{y}_h \end{bmatrix}.$$

The frequency response analysis considers the motion of the system relative to the equilibrium position, hence the constant force terms are neglected. The Laplace Transform of Eqn. (16) produces

$$(sI - \hat{A})Q = (\hat{B}_1 + \hat{B}_2 s)Y_w, \quad (17)$$

$$\frac{Q}{Y_w} = (sI - \hat{A})^{-1}(\hat{B}_1 + \hat{B}_2 s). \quad (18)$$

Q and Y_w are the Laplace transforms of the output and input respectively. The transfer function $\frac{Q}{Y_w}$ is formed by algebraic manipulation of Eqn. (17), and is useful to determine the input-output relationship of the motion of the WEC components.

The symbolic computation is done using the MATLAB symbolic toolbox. This transfer function is defined in the frequency domain by multiplying the displacement transfer function by the derivative operator squared. The transfer function

$$\frac{\Lambda}{Y_w} = s^2\frac{Q}{Y_w}, \quad (19)$$

gives the relationship from the displacement input to the acceleration output. Λ is the acceleration of the system and Y_w is the Laplace transform of the wave input.

2 DEPLOYMENT

The Oscilla WEC first generation prototype was deployed in Lake Washington, by the University of Washington Applied Physics Laboratory. During this 3 month deployment, data was collected for the 3 axis accelerations of the buoy enabling the fundamental means of validating the numerical model of the WEC. Additionally, a load cell in series with the PTO units measured the tension between the PTOs and the buoy. The first three panels in Fig. 3 show a short time span of the raw data collected during the Lake Washington deployment. The deployment data was taken during a winter storm to demonstrate well defined wave characteristics.

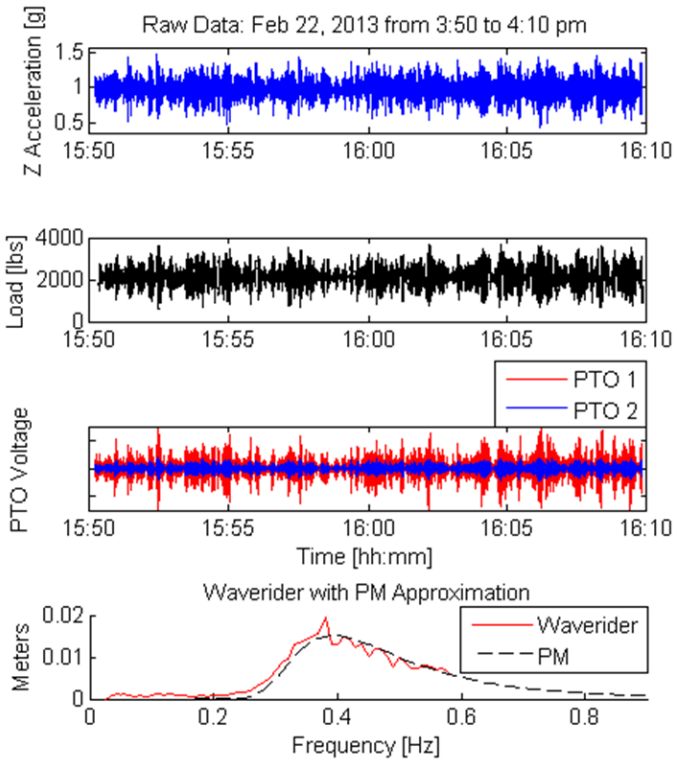

FIGURE 3. Sample raw data from the Oscilla Power wave energy converter generation 1 deployment with measured and approximated incident wave data. Units and y-axis omitted on panel 3 for proprietary reasons.

Lake Washington was a safe testing environment with its relatively calm waters for the vast majority of the time, however during occasional storms the 5 kilometer fetch and increased wind speed allow for more fully developed wave conditions. The deployment occurred at a depth of 52 meters. Incident wave data was taken using a Waverider MK III directional buoy for the duration of the Oscilla Power deployment. Internal to the Waverider buoy, data was processed and stored as a Power Spectral Density (PSD). It is therefore necessary to convert the Waverider PSD data to an amplitude spectrum by multiplying by the bandwidth, then dividing the square root by half to provide valid one-sided amplitude inputs to the simulation used to validate the response of the linear model.

The Pierson-Moskowitz (PM) spectrum is used to model the wave data as a continuous function of frequency. The PM spectrum is a 1 parameter spectrum based on the wind speed in meters per second at 19.5 meters above the steady water line [11]. The PM spectrum is characterized by the assumption that the waves are generated by a steady wind with a very long fetch. The expected spectral amplitude at a given frequency is calculated using

$$E(f) = \frac{0.0081 g^2}{(2\pi)^4 f^5} e^{(-0.74(\frac{2\pi f U_w}{g})^{-4})}, \tag{20}$$

where g is the acceleration due to gravity, 0.0081 is the Phillips constant, f is frequency given in Hz, and U_w is the wind velocity in meters per second at an elevation of 19.5 meters.

In order to determine the wind speed, an optimization function is used to find the wind speed that minimized the error between the PM and the Waverider Spectra. The fourth panel in Figure 3 shows two examples of the best fit PM spectra. While the high peaks in the Waverider data are not captured by the continuous function, the realistic higher frequencies are included. It is important to note that using a JONSWAP spectrum would add an extra parameter providing a more accurate model for fetch limited conditions [11]. However, the experimental conditions are well represented with the more simple PM spectrum.

3 NUMERICAL SIMULATION

The time domain simulation program is implemented in MATLAB to simulate the heave motion of the WEC when subjected to a spectral wave input. The time domain simulation requires time series data for both the displacement and the velocity of the input wave. Since this system involves stiff differential equations, a small time step and a stiff ODE solver is used to simulate the motion of the 3 bodies of the WEC. The acceleration is computed from the simulated displacements and velocities, and the acceleration amplitude spectrum is computed using a Discrete Fourier Transform algorithm.

By using a transfer function, it is possible to compute the acceleration amplitude spectrum given a wave input defined by the PM spectrum by Eqn. (20). This can be compared to the amplitude spectrum of acceleration provided by applying a Discrete Fourier Transform to the vertical acceleration data in Fig. 3. The spectral methods provided excellent validation of the numerical integration of the time series solution.

The dynamics of the WEC are compared using the power spectrum of the acceleration measured in the buoy of the Oscilla WEC. Figure 4 shows the dynamics of the linear model compared to the acceleration response of the deployed system. Once the response of the model was compared against the experimental results a time domain simulation is used to estimate the output of the model as described below. To compute the power spectral density the Fourier coefficients are multiplied by their complex conjugates and then divided by the bandwidth multiplied by two. In this case the bandwidth is $8.56 \cdot 10^{-3}$ Hz and Fig. 4 shows the PSDs as computed using the pwelch function in MATLAB.

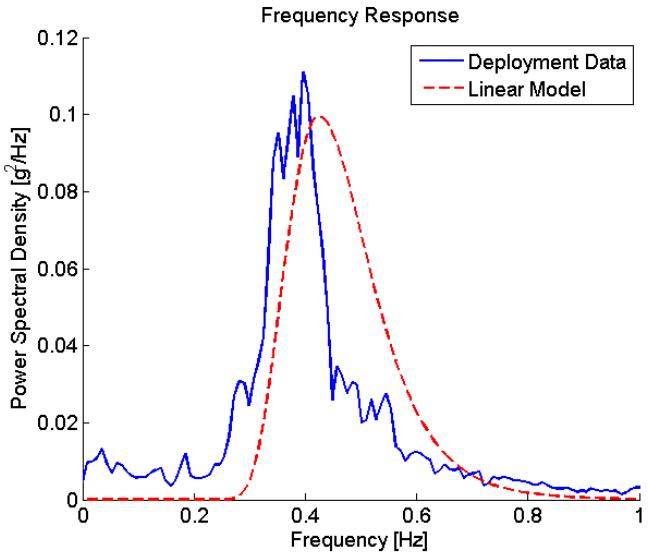

FIGURE 4. Power spectral density of the experimental data and the linear model. The measured acceleration, $\ddot{y}_b$, is the acceleration experienced by the buoy.

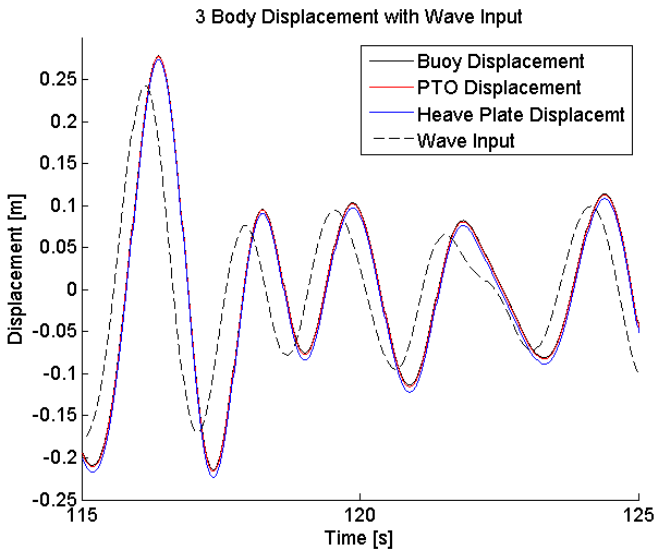

FIGURE 5. Time domain simulation of the relative deflections of the 3 bodies with reference to the wave input, displacement direction is opposite of the convention established in Figs. 1 & 2 for ease of visualization.

3.1 TIME DOMAIN SIMULATION

The time domain simulation of the WEC in response to a wave input is computed by using the stiff numerical integrator ode23s in MATLAB. The PM spectrum of wave amplitudes is used to generate the wave input to the time domain model. Modeling the input wave displacement and velocity by

$$y_w(t) = \sum_{i=1}^{300} a_i \, sin(\omega_i t + \phi_i), \tag{21}$$

$$\dot{y}_w(t) = \sum_{i=1}^{300} a_i \omega_i \, cos(\omega_i t + \phi_i), \tag{22}$$

gives a time domain representation of the wave. Equations (21) and (22) are the sum of 300 sine or cosine waves where the frequencies ω_i are equally spaced, starting at $\omega_1 = 0.15$ Hz and ending with $\omega_{300} = 1$ Hz, and the magnitudes, a_i, correspond to the amplitude of the PM spectrum at the corresponding frequencies, ω_i. The sum is truncated at 300 input frequencies because the variance of the spectrum converges to a constant value. The variable ϕ_i is the phase of each component of the wave spectrum, and is determined by choosing a random phase between 0 and 2π radians. Although real waves do not have a truly random phase, a reasonable time domain input is creating by randomizing the phase for each frequency and amplitude pair.

Figure 5 shows the relative position from the natural length of the connections, illustrating the relative displacement of all three bodies of the WEC compared to the wave input. This enables clear visualization of how the converter is moving when being forced by the incident wave input. As expected, relative positions of the components show that there is never a situation where the connection, holding the components together, is slack which would cause shock loading on the PTO units.

3.2 PREDICTED POWER PRODUCTION

By using the validated model of the motion of the buoy and comparing the predicted PTO output based on the rate of change of tension it is possible to identify the linear proportionality constant α relating the tension derivative to the power production $\mathbb{P} = \alpha \dot{T}$. Here, $\mathbb{P}$ is the power production of the PTO units and $\dot{T}$ is the time rate of change of the tension in the PTO units. Oscilla Power has developed models describing the power production of the magnetostriction based power take off units which are able to production energy from the entire spectrum of the wave input [12].

After identifying the proportionality constant the model is compared against other data sets during the same storm. For reasons of propriety Tab. 1 only shows the error associated with the predicted power.

Table 1 shows the error between the power production from the WEC and the predicted power production from the time domain model. T_D is the dominant period and H_s is the significant wave height of the input. From this table it is shown that the

TABLE 1. Error in the modeled power, Feb. 22, 2013 to Feb. 23, 2013.

Time	T_D [s]	H_s [m]	% Error
22:30-23:00	2.56	0.14	−3.7
23:00-23:30	2.53	0.14	8.2
23:30-24:00	2.58	0.21	7.2
00:00-00:30	2.67	0.21	−8.2
00:30-01:00	2.67	0.28	−10.6
01:00-01:30	2.63	0.28	3.5
01:30-02:00	2.54	0.25	13.3

time domain model has reasonable certainty given the simplified nature of the wave model. The assumption of a purely random phase also adds a small amount of uncertainty when determining the coefficient to predict the power generation of the system.

4 SENSITIVITY ANALYSIS

By using a reference data set it is possible to perform a sensitivity analysis by changing parameters and computing the new power production. The analysis is performed in two stages, first varying each adjustable parameter by positive 5% and then positive 20%.

Table 2 shows the parameters that are varied in the sensitivity analysis along with the corresponding values used in the simulation. It can be seen that the greatest effect on the power production is the mass of the heave plate and the buoyancy of the buoy. This implies that the system is dominated by the inertia of the components and entrained fluid rather than the drag, as may be expected. Despite the great effect the buoyancy of the buoy has on the power production it may be that a disproportionately large buoy is not plausible. The heave plate parameters also have significant impact on the performance of the WEC. Tab. 2 shows that by increasing the mass of the heave plate or by increasing the mass of the fluid entrained by the heave plate the total power production will be increased.

As shown in Tab. 2, a significant change in the estimation of the added mass of the buoy does not produce a significant change in the estimated power production. Likewise, a dramatic increase in both spring constants produces less than a 1.5% change in the power production. A change in the stiffness of the connections between masses can be a result of a change in the spring constant or a change from the modeled 4 meter natural length of the connections. The buoy drag also has a non trivial negative effect on the power generation of the WEC.

TABLE 2. Proportional power change: $\%\Delta\mathbb{P}_1$ is the change in power production when the parameter is changed by +5%, $\%\Delta\mathbb{P}_2$ is the change in power production when the parameter is changed by +20%.

Parameter	Initial Value	$\%\Delta\mathbb{P}_1$	$\%\Delta\mathbb{P}_2$
Buoy mass	570kg	0.3%	0.7%
PTO mass	260kg	1.0%	4.6%
Heave Plate mass	705kg	-0.6%	10.4%
Buoy added mass	220kg	0.5%	0.7%
PTO added mass	10kg	0.5%	0.7%
HP added mass	260kg	1.3%	3.5%
Spring: K_{r1}	1,250,000 $\frac{N}{m}$	0.9%	1.2%
Spring: K_{r2}	270,000 $\frac{N}{m}$	0.2%	0.3%
Buoy buoyancy	22,260$\frac{N}{m}$	3.5%	11.6%
PTO buoyancy	700 N	0.5%	0.3%
HP buoyancy	1000 N	0.5%	0.1%
Buoy drag, D_b	$D_b = 5{,}000\frac{Ns}{m}$	-1.3%	-6.5%
PTO drag, D_p	$D_p = 110\frac{Ns}{m}$	0.8%	-0.0%
HP drag, D_h	$D_h = 1{,}450\frac{Ns}{m}$	-0.1%	-0.6%

In the sensitivity analysis it is important to recognize that the power production is not based on the tension that the PTO units are subjected to, but rather the time rate of change of the tension. Careful consideration should be taken when considering the effect that parameters will have on a point absorber WEC with a different power take out.

5 CONCLUSION

This paper presents an approach to the modeling and validation of a multiple body point absorber wave energy converter. By forming the equations of motions from first principles, rather than using a commercial hydrodynamics package, a model is established for the development of control aimed at reducing the cost of producing energy with arrays of wave energy converters. The equations of motion are developed and then linearized with the goal of validating the amplitude spectrum with experimental data.

Simulations are performed using both spectral and time domain methods using MATLAB to validate the amplitude spectrum of the acceleration of the wave energy converter. After de-

termining a model for the wave input based on incident wave data taken during the deployment, a time domain simulation is used to estimate the power production of the system. A linear proportionality constant is used to relate the time rate of change of tension, applied to the power take off units, to the power generated. The model is then used to compare the predictions with the experimental power production for several different time intervals.

Finally, a sensitivity analysis was used to show that this system is dominated by inertia more than drag. As a result, the design of the system should pay careful attention to the mass of each component and the added mass of the entrained fluid. The heave plate is also shown to be an important component for the performance of the system. The fluid drag and the weight of the heave plate must ensure that the PTO units are never in slack conditions, while not producing an adverse effect on the power production as demonstrated in the sensitivity analysis.

6 FUTURE WORK

Modeling the dynamics of a multiple degree of freedom system will be the first step to model the moorings of marine energy converter arrays. As the foundation to larger simulations, there will be continued research aimed at decreasing the error between the model and deployed wave energy converter. By expanding the model to include the mooring lines additional sensitivity analysis can be performed to identify the performance characteristics of various methods of station keeping.

Point absorber WECs show their greatest potential to be deployed in large energy converter farms [13]. With large numbers of WECs in mind it is necessary to model a network of converters to optimize the performance of a marine energy farm while maintaining the survivability of the converters in extreme conditions. The validated dynamics of a general WEC can now be used to test control methods on a wide variety of wave energy converters.

ACKNOWLEDGMENT

This research was possible as a result of the cooperation between The University of Washington Applied Physics Laboratory, Oscilla Power Inc., and the Northwest National Marine Renewable Energy Center.

This material is based upon work supported by the Department of Energy under Award Number DE-FG36-08GO18179-M001. Recognition of support also goes to the NSF Award: 1230426.

REFERENCES

[1] Johanning, L., Smith, G., and Wolfram, J., 2006. "Mooring design approach for wave energy converters". *Proceedings of the Institute of Mechanical Engineers, Part M: Journal of Engineering for the Maritime Environment*.

[2] Fabien, B. C., 2012. *Nonlinear Approaches in Engineering Applications*. Springer, ch. Equilibrium of a Submerged Body with Slack Mooring, pp. 211–236.

[3] de Andrés, A., Guanche, R., Armesto, J., del Jesus, F., Vidal, C., and Losada, I., 2013. "Time domain model for a two-body heave converter: Model and applications". *Ocean Engineering*(72), pp. 116–123.

[4] Dewhurst, T. e. a., 2013. "Dynamics of a floating platform mounting a hydrokinetic turbine". *Marine Technology Society Journal,* **47**(4), pp. 45–56.

[5] Wacher, A., and Neilsen, K., 2010. "Mathematical and numerical modeling of the aquabuoy wave energy converter". *Mathematics-in-Industry Case Studies Journal,* **2**, pp. 16–33.

[6] Newman, J. N., 1997. *Marine Hydrodynamics*. MIT Pres, ch. 2, pp. 39–45.

[7] White, F. M., 2006. *Fluid Mechanics*. McGraw-Hill Book Company, ch. 7, pp. 450–483.

[8] McCormick, M., 1973. *Ocean Engineering Wave Mechanics*. John Wiley and Sons, ch. 2, pp. 24–35.

[9] Brennen, C., 1982. A review of added mass and fluid inertial forces. Tech. rep., Naval Civil Engineering Laboratory.

[10] Chakrabarti, S., and Cotter, D., 1992. "Hydrodynamic coefficients of a moored semisubmersible in waves". *Journal of Offshore Mechanics and Arctic Engineering,* **114**(1), pp. 9–15.

[11] US ARMY CORPS OF ENGINEERS. *Costal Engineering Manual - Part II, Water Wave Mechanics. pp. 85-92*.

[12] Nair, B. e. a., 2013. "Low-cost utility-scale wave energy enabled by magnetostriction". In Marine Energy Technology Symposium (GMREC), Washington, DC (2013).

[13] Falnes, J., and Hals, J., 2011. "Heaving buoys, point absorbers and arrays". *Phil. Trans. R. Soc. A,* **370**, pp. 246–277.